University of Groningen

INAQS, a Generic Interface for Nonadiabatic QM/MM Dynamics

Cofer-Shabica, D Vale; Menger, Maximilian F S J; Ou, Qi; Shao, Yihan; Subotnik, Joseph E; Faraji, Shirin

[Link to publication in University of Groningen/UMCG research database](#)

INAQS, a Generic Interface for Nonadiabatic QM/MM Dynamics: Design, Implementation, and Validation for GROMACS/Q-CHEM simulations

D. Vale Cofer-Shabica,*,∇ Maximilian F. S. J. Menger,∇ Qi Ou, Yihan Shao, Joseph E. Subotnik, and Shirin Faraji*

ACCESS | 📊 Metrics & More | 📖 Article Recommendations | SI Supporting Information

ABSTRACT: The accurate description of large molecular systems in complex environments remains an ongoing challenge for the field of computational chemistry. This problem is even more pronounced for photoinduced processes, as multiple excited electronic states and their corresponding nonadiabatic couplings must be taken into account. Multiscale approaches such as hybrid quantum mechanics/molecular mechanics (QM/MM) offer a balanced compromise between accuracy and computational burden. Here, we introduce an open-source software package (INAQS) for nonadiabatic QM/MM simulations that bridges the sampling capabilities of the GROMACS MD package and the excited-state infrastructure of the Q-CHEM electronic structure software. The interface is simple and can be adapted easily to other MD codes. The code supports a variety of different trajectory-based molecular dynamics, ranging from Born−Oppenheimer to surface hopping dynamics. To illustrate the power of this combination, we simulate electronic absorption spectra, free-energy surfaces along a reaction coordinate, and the excited-state dynamics of 1,3-cyclohexadiene in solution.
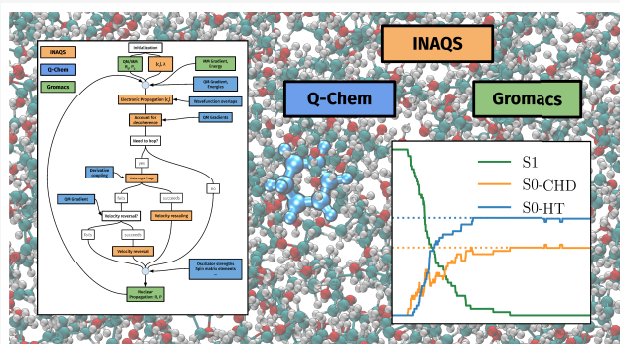
1. INTRODUCTION

The accurate description of large supramolecular and solvated systems presents a considerable challenge in the field of computational chemistry. Given the inherent electronic structure difficulties of modeling bond-breaking and charge reorganization in vacuum, it follows that modeling such processes in the presence of a complex environment can be quite difficult. In the case of extended systems, a complete quantum description is still not feasible today; even in light of the algorithmic and computational advances promised by new computational schemes[1−4] and GPU acceleration.[5−7] Luckily, for many chemical processes of interest, quantum effects occur within a spatially localized region; and for such systems— provided the dynamics occur along the electronic *ground state*—there does exist today an enormous quantum mechanics/molecular mechanics (QM/MM) computational infrastructure.

At the frontier of modern QM/MM software is the study of nonequilibrium processes, especially nonadiabatic *excited-state* molecular dynamics (e.g., photoreactions in light-harvesting complexes[8−11]) in the presence of a complex environment.[12] For excited-state problems, the role of the environment is even more important than for the ground state. After all, photochemical processes can release a great deal of energy that must be dissipated or marshaled by the environment.

Unfortunately, however, when simulating nonadiabatic dynamics with a strongly interacting environment, new theoretical issues do arise. To see this point, consider a typical system with heavy nuclei and light electrons. For such a system, one can safely assume the electrons move with nuclei frozen or quasi-frozen, but the perennial question in non-adiabatic dynamics is how does one move the *nuclei* if one does not know the correct electronic state to move along? Within the context of QM/MM approaches, this question must then be superimposed with yet another question: how does one best move the nuclei of the system in the presence of solvent nuclei? In short, the presence of QM/MM interactions introduces more time scales and potentially more questions to a nonadiabatic dynamics problem.

The answers to these questions are inevitably dependent on what level of theory one considers and what approximations one is willing to make. As far as treating the solvent
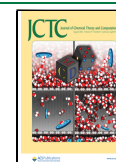
environment, there are basically two approaches, implicit and explicit:

- *Implicit* models, such as the polarizable continuum model (PCM),[13−15] the conductor-like screening model (COSMO),[16,17] or SMx models,[18,19] describe the environment in terms of a continuous medium. These approaches are very computationally efficient and best-suited for situations where the environment is homogeneous since a detailed molecular structure of the solvent is not given. To date, however, safely merging nonadiabatic dynamics with implicit solvation models remains a theoretical challenge. For instance, most semiclassical approaches for nonadiabatic dynamics rely on a time scale separation between slow nuclei and fast electrons; but for PCM models, one assumes the solvent response is also very fast, which can complicate the necessary dynamical question.

- *Explicit* QM/MM solvation approaches directly include individual solvent molecules in the simulation, often through classical force fields (FFs) and molecular mechanics (MM). These approaches are more computationally expensive than the implicit models, because of their sampling requirements, but can better treat heterogeneous environments and situations where the coupling between the active site and environment is dependent on the relative orientation or position of the active site and the immediate environment. Moreover, because one treats system nuclei and solvent nuclei at the same level of theory, there are fewer theoretical challenges, with regard to implementing nonadiabatic semiclassical dynamics algorithms.

Now, the tradeoff for substituting explicit for implicit QM/MM models is that one trades in theoretical problems for practical questions: How can one accurately treat the interaction between QM and MM subsystems?[8,20−27] How should one treat the boundary, especially when a covalent bond bridges the interface?[28−30] A successful QM/MM software package must combine complicated electronic structure and molecular mechanics dynamics calculations, and problems often arise when there is tight coupling between the different components; moreover, a useful software package must be well-structured, adaptable, and highly efficient given the large spatial scales of the systems of interest and the need to propagate simulations lasting long times.

With these general concerns in mind, the existing QM/MM implementations can be roughly divided into three different broad categories:

(1) **QM Driver**: A straightforward approach to QM/MM simulations is to implement all the necessary code within an existing electronic structure software package (e.g., Q-Chem,[31] Gaussian[7]). Here, the main driver is the QM code, which requires an internal implementation of MM force fields and any dynamics desired. In these cases, the focus is typically on the description of the QM subsystem and optimizations or scans can use specialized approaches, such as the microiteration scheme.[32] Molecular dynamics (MD) is generally not the main focus and the statistical capabilities are often less comprehensive than in MD codes.

(2) **MD Driver**: Another approach is to implement the necessary code as part of an existing MD code, such as GROMACS,[33] NAMD,[34] AMBER,[35,36] or CHARMM.[37]

Here, the QM contributions are typically provided by an interface to external electronic structure codes. This approach is built around the MD capabilities of the MD codes and enables advanced sampling techniques for various ensembles and QM/MM dynamics. Features for static calculation, such as optimizations or transition-state searches, are often limited, although in the condensed phase, they are of questionable utility.

(3) **Standalone**: A third approach is a fully independent implementation that involves constructing a new program that collates the outputs of existing QM and MM codes to build up a QM/MM calculation. This is immensely flexible, because the developer has full control over the capabilities and can interface with whatever QM and MM codes she or he chooses. However, that flexibility comes at a price: the developer must reimplement any desired features for dynamics, optimization, or statistics. Examples of such hybrid software packages include ChemShell,[38−40] CobraMM,[41,42] QMMM,[43] SHARC,[44,45] and Newton-X.[46,47]

To date, for ground-state properties, a large variety of implementations exist employing all three of the above approaches. For excited-state properties, especially when nonadiabatic effects must be taken into account, most implementations follow either the QM driver (1) or standalone (3) schemes. In particular, for nonadiabatic dynamics, including solvent effects, the electronic properties (e.g., energies, gradients, nonadiabatic couplings) are typically computed via the standalone approach.[45,47−53] To the authors' knowledge, and with the exception of some in-house codes,[54,55] integrating the nonadiabatic effects into an existing MD code (2) is rarely employed.[56] But, this approach has several distinct advantages: reduced data transfer and efficient schemes for storing and analyzing long trajectories; the widespread availability of established force fields for all types of solvents; and the use of advanced sampling and metadynamic schemes.

With all of this background in mind, here we present INAQS (Non-Adiabatic Quantum mechanics/molecular mechanics in Solvent), which is a new interface for nonadiabatic QM/MM dynamics following approach (2). INAQS links the MD code Gromacs to the electronic structure software Q-Chem and enables ground- and excited-state ab initio molecular dynamics (AIMD), nonadiabatic surface hopping and Ehrenfest dynamics, and enhanced sampling within the mechanical or electrostatic embedding QM/MM framework. Below, we present the software implemented, a few applications to single-state dynamics, and results from multistate fewest switches surface hopping (FSSH) algorithm-solvated trajectories. An outline of this paper is as follows. In Section 2, we discuss the theory of additive QM/MM with electrostatic embedding, nonadiabatic dynamics, and the implementation choices made in INAQS. In Section 3, we demonstrate INAQS' capacities for AIMD and QM/MM umbrella sampling. In Section 3.3, we present surface hopping results. We conclude this work in Section 4.

2. THEORY

2.1. The QM/MM Hamiltonian. In QM/MM schemes, like other hybrid quantum/classical approaches,[8,15,57] the total energy of the system, S, can be written as the sum of the

energy of the QM inner subsystem $\mathcal{I}$, $E_{QM}(\mathcal{I})$, the MM energy of the environment (outer subsystem) O, $E_{MM}(O)$, and their interaction, $E_{QM-MM}(\mathcal{I}, O)$:[58]

$$E(\mathcal{S}) = E_{QM}(\mathcal{I}) + E_{MM}(O) + E_{QM-MM}(\mathcal{I}, O) \tag{1}$$

The MM region is described by a classical force field generally composed of harmonic bonded interactions (bonds, angles, and dihedrals) and Coulomb and Lennard-Jones interactions for the nonbonded interactions. The QM region is computed with an appropriately chosen electronic structure method. In mechanical embedding, all interactions between the QM and the MM region are treated at the MM level of theory and the QM contribution to the total energy is obtained by performing a vacuum calculation on QM region. Thus, no polarization of the QM system arises due to the environment. The electrostatic interactions between the QM and MM regions are treated purely classically, in terms of the Coulomb interaction of fixed point charges, which can be a problem, especially if the system undergoes a chemical reaction that significantly changes its electronic density.

The missing polarization of the QM region in the mechanical embedding can be addressed by the electrostatic embedding scheme, where the nonbonded electrostatic interactions between QM and MM region are treated at the QM level of theory. Nonbonded, nonelectrostatic interactions (Lennard-Jones) are still computed classically.

Because of the inclusion of the charges of the MM region into an effective interaction Hamiltonian, the environment is able to polarize the electronic density:

$$\hat{H}^{eff}|\Psi\rangle = (\hat{H}^0 + \hat{H}^{QM-MM})|\Psi\rangle = E|\Psi\rangle \tag{2}$$

Here, H^0 is the Hamiltonian of the isolated QM subsystem, $E_{QM}(\mathcal{I})$, and H^{QM-MM} is the electrostatic coupling between the inner and outer subsystems. For the electrostatic embedding, this interaction operator is given by an additional nuclear-like one-electron term in the Hamiltonian:

$$\hat{H}^{QM-MM} = \sum_k \frac{q_k}{|\vec{R}_k - \hat{\vec{r}}_1|} \tag{3}$$

where q_k is the charge of the MM atom k at position $\vec{R}_k$. When computing the resulting forces on the MM atoms, one simply takes the product of the charge on the MM atom and the electric field arising from the electronic density and QM nuclear charges evaluated at $\vec{R}_k$:

$$\vec{F}_k = q_k \vec{E}(\vec{R}_k; \rho) \tag{4}$$

This approach can be easily generalized to excited states. As one should expect, our interface, which implements an electrostatic embedding, can produce a mechanical one "for free" simply by turning off the one-electron terms and turning the classically computed electrostatics back on.

INAQS does not currently support polarizable embeddings, which is certainly a limitation of the platform, since solvent electronic response can be important, e.g., for absorption spectra. That being the case, as far as nonadiabatic dynamics is concerned, it is also well-known[59] that one cannot simply include the "electronic reorganization energy" (generated by a polarizable force field) within the adiabatic potential energy surfaces. After all, as shown convincingly in ref 59, Marcus theory is predicated on the idea that the solvent response is

slow (which corresponds to the solvent nuclear response). If one were to consider the electronic response of the solvent, one could not make the quantum-classical separation that we do when running surface hopping (or any semiclassical dynamics); one cannot safely presume that the solvent electrons would respond more slowly than then quantum molecular electrons. From a surface hopping point of view, it follows that if we are to include a polarizable solvent force field, we will also need to calculate the corresponding changes to the derivative couplings. This feature (while very important) will need to be addressed in a future report.

2.2. Excited-State Dynamics. INAQS models the excited-state nonadiabatic dynamics of medium to large molecular systems in solvated environment using linear-response Ehrenfest (as opposed to real-time Ehrenfest) dynamics or fewest switches trajectory surface hopping[60] dynamics. Since the physics of Ehrenfest[61] and surface hopping[62] dynamics are well-described in the literature, here we will only briefly describe the theory behind these methods, before describing in detail the practical numerical issues that go along with the INAQS implementation.

For both linear response Ehrenfest and surface hopping dynamics, the nuclear and electronic degrees of freedom are propagated separately. Propagation of the electronic degrees of freedom is straightforward. The electronic degrees of freedom are represented by a time-dependent electronic wave function Ψ^{elec}, expanded in a known set of basis functions Φ_i:

$$\Psi^{elec}(t) = \sum_i c_i(t)\Phi_i(\vec{R}(t)) \tag{5}$$

Here, $\vec{R}(t)$ is the time-dependent vector of nuclear positions. The set $\{\Phi_i(\vec{R}(t))\}$ are typically selected as the wave functions of the adiabatic states of the system, which are implicitly dependent on time through $\vec{R}(t)$, and the $c_i(t)$ denote the corresponding time-dependent weights of each state i. The electronic wave function Ψ^{elec} is propagated using the time-dependent Schrödinger equation,

$$i\hbar\frac{\partial}{\partial t}\Psi^{elec}(t) = \hat{H}^{elec}\Psi^{elec}(t) \tag{6}$$

with $\hat{H}^{elec}$ being the electronic Hamiltonian of the system and $\hbar$ being the reduced Planck constant. In a moving basis (e.g., the adiabatic basis), this equation reduces to a standard set of coupled equations for the expansion coefficients $c_i(t)$,

$$i\hbar\dot{c}_i = \sum_j c_j[V_{ij} - i\hbar\dot{\vec{R}}\cdot\vec{d}_{ij}] \tag{7}$$

where the $V_{ij} = \langle\Phi_i|\hat{H}^{elec}|\Phi_j\rangle$ are the matrix elements of the electronic Hamiltonian, and $\vec{d}_{ij} = \left\langle\Phi_i\left|\frac{\partial}{\partial\vec{R}}\right|\Phi_j\right\rangle$ are the non-adiabatic coupling vectors between adiabatic states Φ_i and Φ_j. Within INAQS, eq 7 is integrated via matrix exponentiation in order to propagate the expansion coefficients from t to $t + dt$.

This completes the straightforward electronic propagation. The propagation of the nuclei is more demanding and requires a strong semiclassical approximation: one based either on mean-field Ehrenfest dynamics or on state-specific surface hopping dynamics. Generally, the nuclei follow Newton's equation of motion:

$$\mathbf{M}\ddot{\vec{R}} = -\vec{\nabla} E_\lambda \tag{8}$$

where M is the diagonal matrix of masses of all nuclei and E_λ is the energy of an electronic state λ. The key question is the definition of λ.

2.2.1. Ehrenfest Dynamics. Ehrenfest dynamics is a mean-field theory that is most accurate when (i) the adiabatic surfaces of interest, are nearly parallel (so that moving along an average surface makes a lot of sense);[63] or (ii) when the nuclear motion is fast and there is less separation between nuclear and electronic time scales (an extreme case being classical photon−quantum electron interactions[64]). Over the years, a host of nonadiabatic dynamics based on the Ehrenfest equations of motion (but improved upon by using different quasi-classical initialization schemes) have been developed.[65−67] For now, INAQS has implemented only standard Ehrenfest dynamics based on simple classical sampling of the initial conditions.

Mathematically, for Ehrenfest dynamics, the effective energy is the average energy:

$$E_\lambda = \sum_{ij} c_i^* V_{ij} c_j \tag{9}$$

One must be careful when differentiating this expression. For linear response Ehrenfest dynamics expressed in an adiabatic basis of electronic states, the correct force is

$$\ddot{\vec{R}} = -\mathbf{M}^{-1}\left(\sum_i |c_i|^2 \vec{\nabla} V_{ii} - \sum_{ij} c_i^* c_j \vec{d}_{ij}(V_{jj} - V_{ii}) \right) \tag{10}$$

where we note that the last term in parentheses is real-valued and equivalent to $\sum_{ij} \Re[c_i^* c_j]\vec{d}_{ij}(V_{jj} - V_{ii})$.

2.2.2. Surface Hopping. Surface hopping takes a different approach from Ehrenfest dynamics and propagates nuclei on one "active" adiabatic surface (with the possibility of hops to another adiabatic surface). Because nuclei usually move far slower than electrons, for molecular systems, trajectory surface hopping usually has a greater regime of applicability than Ehrenfest dynamics. The former method also recovers detailed balance,[68,69] unlike the latter (although some advances have been made recently[70]).

There are many subtleties associated with the implementation of surface hopping in practice. The implementation in INAQS largely follows Jain and co-workers[71] with some modifications. The salient features are as follows:

(1) The wave function is propagated following eq 7 via an extended Meek and Levine overlap scheme[71,72] that significantly extends the time step from the original finite difference approach suggested by Hammes-Schiffer and Tully.[73,74] In brief, we take

$$\dot{\vec{R}}\cdot\vec{d}_{ij} = \frac{1}{dt}(\log \mathbf{U})_{ij}$$

where $(\mathbf{U})_{ij} = \langle \Phi_i(t)|\Phi_j(t + dt)\rangle$. According to this expression, we effectively average the nonadiabatic coupling term over the duration of the entire classical time step. Maintaining the orthogonality while computing the matrix logarithm of a unitary matrix is nontrivial and, thus, we employ a technique based on the Schur decomposition.[75] With this simplification, nonadiabatic coupling vectors do *not* need to be computed at every time step, but rather only when there is a transition. Note that in Figure 1 the computationally less demanding right "no" branch is most often followed afterward by 'Need to hop?'. Highly efficient, exact matrix overlaps for spin-flip CIS and TD-DFT states have recently been implemented in Q-Chem.[76]

(2) Since the phases of the wave functions are undefined, the signs of the columns of $\mathbf{U}$ are also formally undefined. For smooth dynamics, one can always choose the diagonal elements to be positive (so-called "parallel transport"); however, in the presence of trivial crossings[77,78] (particularly sharp crossings where the diabatic coupling is nearly zero and a hop guaranteed), such a scheme is ill-behaved. To that end, INAQS implements the protocol outlined by Zhou and co-workers[77] that aims to pick adiabatic signs by minimizing a surrogate for the function $\mathrm{Tr}[|\log \mathbf{U}|^2] \approx \mathrm{Tr}[3\mathbf{U}^2 - 16\mathbf{U}]$.

(3) For velocity reversal, we follow Jasper and Truhlar,[79] reversing the nuclear velocity along the direction of the nonadiabatic coupling vector whenever a hop fails and $-\vec{\nabla} V_j\cdot\vec{d}_{\lambda j}\vec{d}_{\lambda j}^T \mathbf{M}^{-1}\dot{\vec{R}} < 0$; i.e., when the momentum projected along the nonadiabatic coupling vector opposes the force from the surface that the system failed to reach. This protocol was found to be superior[80] to that suggested in ref 71.

(4) Decoherence certainly can play an essential role in surface hopping. For instance, it is known that, in some regions, surface hopping recovers incorrect scaling laws for the Marcus problem.[81,82] Nonadiabatic transition-state theory can also suffer without decoherence.[83] INAQS has implemented a module for decoherence, and we will report the effects and necessity of decoherence effects in the condensed phase in a later publication.

2.3. Code Infrastructure. Born−Oppenheimer, Ehrenfest, and surface hopping dynamics all propagate Newton's equations and conserve energy. In developing INAQS, we sought to exploit this conservation law to develop an interface with minimal intrusion on the MD driver. In practice, trajectory-based MD simulations can be crudely divided into two parts: (i) a nuclear propagator that determines the next position of the nuclei in time by integrating a given force and (ii) a force provider that computes molecular gradients for the given nuclear (and possibly electronic) configuration.

Let us first consider the role of the force provider for each specific dynamics scheme considered above. In the case of purely classical MD, the gradient is obtained via a (predetermined) classical force field, typically representing the ground electronic state. For single-state Born−Oppenheimer dynamics, the force provider computes a gradient for a fixed electronic state. For Ehrenfest dynamics or surface hopping, however, the forces are dependent on the excited electronic states and, for each method, there is a different gradient. For Ehrenfest dynamics, the force provider must pass a gradient that incorporates knowledge of the corresponding electronic wave function and (for linear-response dynamics, as opposed to real-time Ehrenfest dynamics) also the non-adiabatic couplings between the electronic states (see eq 10). For surface hopping dynamics, the provider must pass an electronic state gradient that incorporates all hopping information.

Second, let us address the nuclear propagator within the MD code. The nuclear propagator receives the forces and integrate
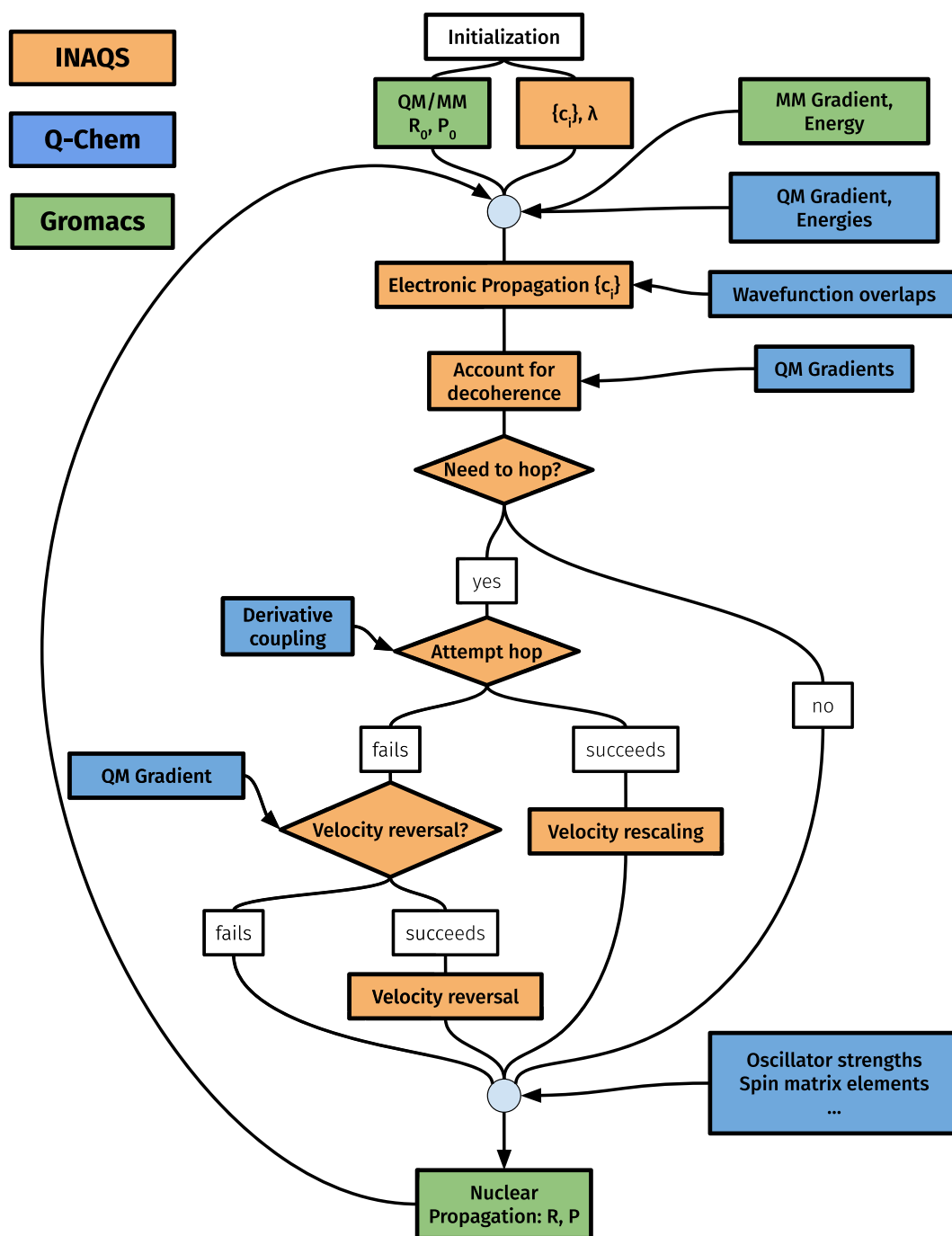
Figure 1. Fundamental steps of a surface hopping molecular dynamics simulation. INAQS (in tan/orange) acts as an interface between the electronic structure software (Q-Chem, in blue) and the MD driver (Gromacs, in green) to track and integrate the electronic wave function, provide relevant electronic properties of the system, and effect velocity rescaling or reversal during a hopping event. INAQS hooks into Gromacs at exactly 2 points: once to supply QM energies and gradients (as is typical in an MD code) and again to optionally update velocities during a hopping event. The code is quite general and we support single-state calculations or Ehrenfest dynamics via the same codepaths.

Newton's eqs (eq 8) to determine the new positions and momenta. Generally, the nuclear propagator does not care how the forces are obtained—whether from force fields (molecular mechanics), an electronic structure calculation, or a hybrid QM/MM setup. One may even apply ab initio exciton or fragment-based Hamiltonians.[52,84–86] Thus, generally, a call to update the nuclear position should be valid across a variety of different algorithms from classical MD to ab initio MD to Ehrenfest dynamics and surface hopping. There is one difference between surface hopping and the other algorithms presented above; following Pechukas[87] and Herman,[88] in the case of a hop, the velocities of the system must be rescaled to conserve the total energy. Even so, a carefully designed interface can be quite simple and very general. The decoupled nature of the nuclear and electronic propagation schemes allows a variety of trajectory-based MD approaches to be implemented by way of the same code paths.

In practice, implementing surface hopping within an existing MD code is more difficult than Ehrenfest dynamics, because of the new functionality required to conserve energy when
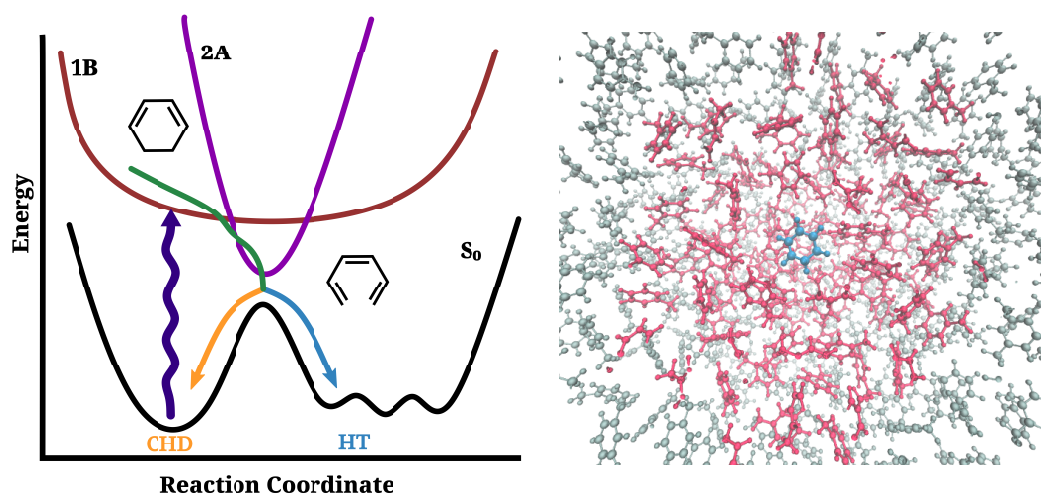
Figure 2. (Left) Schematic of the photo excitation and relaxation process for CHD. (Right) Snapshot from the dynamics trajectory. The central, blue molecule is CHD and has been treated with ab initio forces; the surrounding molecules are toluene, described via a classical force field; the nearer ones, in red, are mobile; those molecules farther away, in gray, are constrained to be frozen.

changing surfaces or reversing the velocities, and so we will focus on the former here. The basic scheme for surface hopping is presented in Figure 1. The INAQS software implements function calls in two places within the GROMACS MD package.

2.3.1. GROMACS Interface. The current implementation of INAQS is tied to a modified version of the Gromacs, which implies that one requires all of the usual inputs as appropriate for a classical MD simulation. The INAQS and GROMACS codes are linked together at the source level to allow direct memory access for communication. Similarly to many MD codes,[89] Gromacs preferentially uses a leapfrog integrator. Such an integrator is not usable for surface hopping, because velocities and positions are not obtained for the same time, but rather interleaved. Velocity-Verlet is available within Gromacs, but is implemented using the same code-paths as leapfrog.

INAQS requires only two function calls be inserted into Gromacs (or any other MD program):

(1) The first call computes QM energies and forces.
(2) The second call updates velocities and the gradient in the event of a hop.

To understand where these two calls are placed exactly, consider the structure of the existing GROMACS integrator. At the start, a force is required to propagate the current nuclear coordinates:

$$\vec{F}(t) = -\vec{\nabla} V|_{\vec{R}(t)} \tag{11}$$

A standard Gromacs code computes the MM forces and Q-Chem computes the QM energies, forces, and any other requested properties.

First call: INAQS constructs the necessary input for Q-Chem and returns the results via Gromacs' additive QM/MM routines to update the force. During this time, INAQS also integrates eq 7 for the electronic coefficients and determines if a hop is necessary.

The next step in the Gromacs' MD routine is the first velocity half-step:

$$\vec{v}(t) = \vec{v}\left(t - \frac{\Delta t}{2}\right) + \mathbf{M}^{-1}\vec{F}(t)\frac{\Delta t}{2} \tag{12}$$

Second call: After eq 12, INAQS determines whether or not a hop should occur and implements velocity rescaling and/or reversal. If the code determines that a hop succeeds, we modify the velocities using the usual energy conservation equations, and then update Gromacs' QM potential energy and gradient.

At this point, Gromacs enforces any applicable constraints via SHAKE, RATTLE, and/or LINCS; note that, having adjusted the potentials and velocities *beforehand*, INAQS is compatible with such constraints.

Finally, Gromacs takes its second velocity half-step:

$$\vec{v}\left(t + \frac{\Delta t}{2}\right) = \vec{v}(t) + \mathbf{M}^{-1}\vec{F}(t)\frac{\Delta t}{2} \tag{13}$$

and updates the nuclear positions:

$$\vec{x}(t + \Delta t) = \vec{x}(t) + \vec{v}\left(t + \frac{\Delta t}{2}\right)\Delta t \tag{14}$$

The INAQS repository contains a locally modified version of Gromacs 4.6.5 implementing these changes. INAQS is compatible with enhanced sampling protocols like umbrella sampling via Gromacs's native algorithms or PLUMED2[90] (which also connects to Gromacs). INAQS uses atomic units exclusively internally; conversion to and from the MD code's unit system is performed automatically.

2.3.2. Q-CHEM Implementation. While INAQS is relatively decoupled from Gromacs on the MD side, the interface to Q-Chem is much more extensive. This extra coupling is a result of the fact that many more choices must be communicated to the electronic structure software (basis sets, functionals, convergence algorithms), as opposed to the MD software (which, by design, mostly handles itself). Communication with Q-Chem is handled via a system call rather than direct linking, but INAQS directly reads the binary intermediaries (rather than parse any ASCII output). The Q-Chem execution environment is established in the usual way with Q-Chem's standard environmental variables, indicating the location of the executable and scratch directories. INAQS allows the user to control the number of threads used for parallel execution (see Section 3 of the Supporting Information for an example input file). Calls to Q-Chem are heavily optimized to avoid recalculation of the SCF or excitation amplitudes while
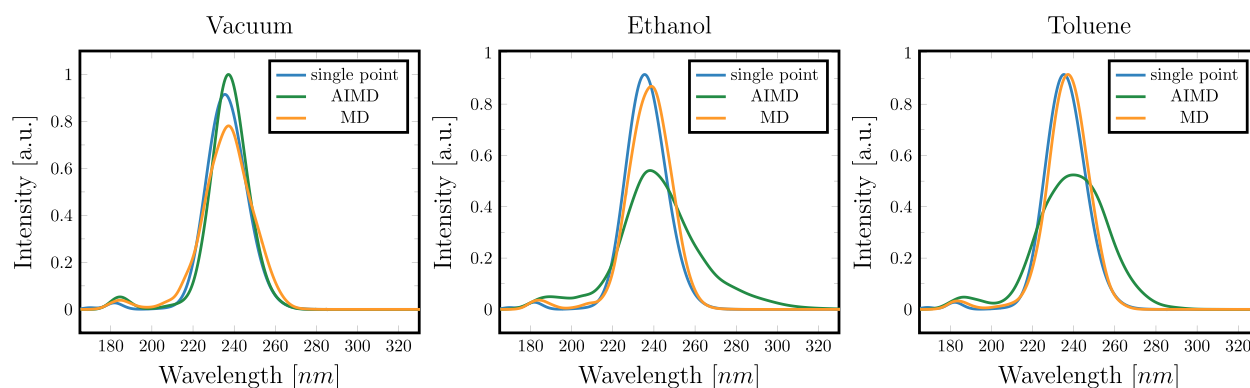
Figure 3. Absorption spectrum of the CHD simulated from (i) a single point calculation of the ground-state equilibrium with a CPCM implicit solvent model (single point, blue), (ii) snapshots taken from classical MD simulations with explicit inclusion of the solvent molecules (MD, orange), and (iii) snapshots from structures obtained from ground-state AIMD (AIMD, green) via electrostatic embedding.

maintaining flexibility in the types of properties that we compute. In practice, we find that, per geometry, the INAQS implementation is 2−3 times faster than naive job submission would be (see Section 1 of the Supporting Information for explicit performance data). INAQS is compatible with Q-Chem versions 5.4 and higher in their unmodified state. Spin-flip overlaps for spin-flip nonadiabatic dynamics are implemented starting in Q-Chem version 6.0.

2.3.3. Availability. INAQS is written in the C++11 programming language and provides an easy-to-use C (specifically C89) interface, allowing compatibility with almost all programming languages and existing software packages. The source code is available on GitHub at github.com/INAQS/inaqs. INAQS is written in a modular way such that the code can be easily adapted to another MD package that uses the velocity-Verlet algorithm. In principle, one can also change electronic structure software as long as the new package can evaluate the overlap of electronic wave functions.

3. APPLICATIONS

The photochemical interconversion between 1,3-cyclohexadiene (CHD) and hexatriene (HT) is a common example of a (4n+2) photo electrocyclic reaction, following the Woodward−Hoffmann rules (see Figure 2) and has been intensively studied[91] both experimentally[92−94] and theoretically.[95−97] Generally, there is widespread interest in the structure and dynamics of CHD and substituted CHD, since this class of molecules plays a crucial role in many biological processes— e.g., the photobiological synthesis of vitamin D3—and also is a target platform for the design of molecular photoswitches. That being said, photochemistry and photoswitches do not operate in a vacuum, but rather in complex environments (e.g., solvent) and it is essential to account for a solvent if one seeks an accurate description of such processes. In this section, we will present the following: (i) the absorption spectrum of CHD in different solvents (toluene and ethanol), as computed by Born−Oppenheimer AIMD trajectories; (ii) the free-energy profile of the ring opening reaction, i.e., CHD to HT conversion, as computed by umbrella sampling; and (iii) photochemical dynamics of the excited state ring opening, as computed by surface hopping calculations. Most of these applications are not new[4,47,98] per se, but are offered as a means of highlighting the capabilities of INAQS.

3.1. Absorption Spectra. The photoabsorption spectrum of the CHD is simulated using vertical excitation energy

calculations obtained from three different approaches; (i) single-point calculation of the ground-state equilibrium with implicit solvent model (CPCM), (ii) 2000 snapshots taken from a 2 ns classical NVT MD simulation with explicit inclusion of the solvents (ethanol or toluene molecules), (iii) 2 × 10^4 structures obtained from a 20 ps ground-state AIMD simulation via electrostatic embedding. To investigate the extent to which the absorption spectra are influenced by the presence of the implicit and/or explicit solvent models, we also simulated the absorption spectrum for all three approaches in vacuum. Absorption spectra were obtained as a normalized superposition of Gaussians localized at computed excitation energies (ϵ_i),

$$I(\epsilon) \propto \sum_i f_i/\sigma \exp\left[-\frac{(\epsilon - \epsilon_i)^2}{\sigma^2}\right]$$

(15)

with f_i being the oscillator strength and σ the spectral broadening. Spectra are normalized to have a constant absorption cross section, i.e., $\int_{-\infty}^{\infty} I(\epsilon)\, d\epsilon = 1$. The broadening ($\sigma$) is chosen to be 0.1 eV for approaches (ii) and (iii) and 0.3 eV for approach (i); the latter broadening parameter must be larger than the former in order for the different methods to match; after all, only the former includes inhomogeneous broadening.

In all three approaches, the spectrum is dominated by the first bright excited state with an excitation energy of ~5.3 eV. As it is evident from Figure 3, the inclusion of the solvent has no significant effect on the position of the peak maximum (~0.05 eV). This lack of change should not be surprising, as CHD is a small rigid molecule that oscillates mainly around its ground-state equilibrium structure. Note that the classical, quantum mechanically derived force field does capture the correct ground-state potential energy landscape for the MD simulation of the isolated CHD. However, the method fails to capture the polarization of the QM region in the presence of the explicit solvents. This failure can be seen by comparing the spectra obtained using ground-state AIMD and MD for isolated CHD and solvated CHD in Figure 3; the spectrum obtained via ground-state AIMD results in a significantly broader spectrum when the explicit solvents are present (with toluene showing a slightly larger broadening), while both methods result in approximately the same spectrum for the isolated CHD.
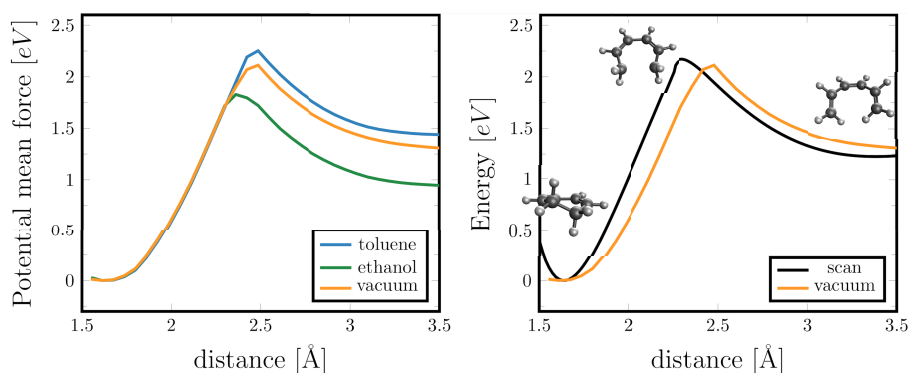
Figure 4. (Left) Potential of mean force along the reaction coordinate of the ring opening of CHD in different environments toluene (blue), ethanol (green), and the isolated molecule (orange). (Right) Vacuum comparison between the potential of mean force (orange) and the relaxed surface scan using Q-Chem (black) for CHD.
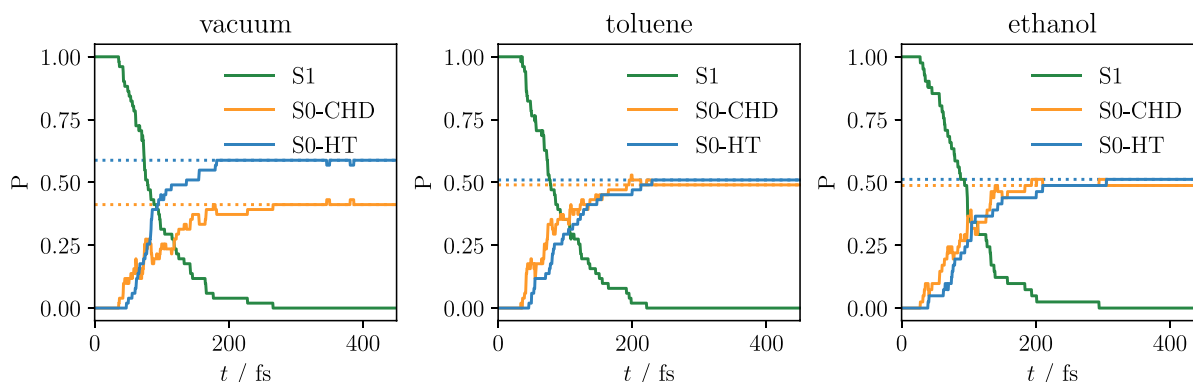

Figure 5. Evolution of the populations of the electronic states during surface hopping dynamics for the three simulations in vacuum, in toluene, and in ethanol. The S_1 state (green) rapidly decays and transfers population to the ground state S_0, where two different products will be formed, namely, the closed-ringed cyclohexadiene (CHD) (orange) and open hexatriene (HT) (blue). Initial excited-state structures were drawn from ground-state AIMD simulations, as described in Section 1 of the Supporting Information.

The observations above lead us to hypothesize that the presence of solvent mainly modifies the *ground-state* potential energy landscape, while the vertical excitation energies are only marginally affected within electrostatic embedding. To further confirm this hypothesis, we calculated the RMSD for the excitation energies computed with and without the explicit solvent for 2000 structures, which is found to be ∼0.01 eV for the first 10 excited states. However, the energetic fluctuations due to structural changes obtained from calculations with explicit solvent are an order of magnitude larger (∼0.2 eV) than the excitation energy RMSD. Thus, we conclude that the spectral broadening in the AIMD of solvated CHD is mainly attributed to structural fluctuations in the ground state.

3.2. Umbrella Sampling. Using INAQS, we have modeled the thermally induced ring-opening reaction (CHD to HT) in the ground state (see Figure 2), using umbrella sampling.[99,100] The free-energy landscape is computed along the ring-opening reaction coordinate within an electrostatic QM/MM embedding (see Section 1 of the Supporting Information for computational details).

The distance between the center of mass (COM) of the two CH$_2$ groups of the CHD is chosen as the pulling coordinate. First, a single pull is performed to sample the initial structures for the windows of the umbrella sampling; a 10 ps MD run is performed with a pulling rate of 0.5 Å/ps along the ring-opening coordinate, ranging from 1.5 Å (closed) to 3.5 Å (open). For this trajectory, the molecule is driven quickly

enough such that the environment may not have time to fully relax. Second, and subsequently, a 2 ps MD simulation with fixed harmonic constraint for the reaction coordinate was performed in 0.1-Å-wide windows starting from three selected structures from the initial pulling simulation. The free-energy profile for different solvents are shown in Figure 4 and compared to the potential energy curve obtained by a relaxed surface scan of the isolated CHD using Q-Chem along the C−C bond distance. In all cases, the maximum of the potential is found to be located at ∼2.4 ± 0.1 Å of the CH$_2$−CH$_2$ COM distance, with toluene showing the smallest distance, ethanol the largest, and isolated CHD being in the middle. It is worth mentioning that the barrier in ethanol is lowered by 0.5 eV and the open ring form (HT) is stabilized by 0.5 eV, compared to the toluene case. The energy profile obtained using umbrella sampling of the isolated CHD agrees well with the relaxed surface scan (subfigure on the right in Figure 4). The high energy barrier observed in the ground state (more than ∼42 kcal/mol = 71$k_B T$) prevents thermal interconversion between the closed-ring and open-ring forms.

3.3. Surface Hopping. There is extensive experimental[94] and theoretical[97] literature[91] exploring the photoinduced ring opening dynamics of CHD. The basic physics is that the ground-state functions as a double well with CHD and HT as two stable isomers. Upon photoexcitation, there are two excited states of interest: a singly excited state (often referred to as 1B) and doubly excited state (often referred to as 2A).

Conical intersections can be identified between the 1B and 2A excited states, as well as between the 2A and S_0 ground state. For a schematic, see Figure 2.

As described in Section 1 of the Supporting Information, we have now run surface hopping calculations at the level of spin-flip TD-DFT for CHD. While our calculations do not resolve a 1B−2A conical intersection (and the calculations do suffer from spin contamination[101]), we do resolve a strong transition (likely a conical intersection) when we monitor the transition from the first excited putative singlet state, S_1, to the ground state. In principle, one goal of QM/MM dynamics is to identify the molecular characteristics that guide a reaction to form either HT (S_0-HT) or relax back to CHD (S_0-CHD) in solution.

In Figure 5, we plot the population transfer for CHD simulations in three different environments: the isolated molecule (vacuum), in toluene, and in ethanol. The overall population transfer is quite similar in all cases, where an ultrafast (within the first 200 fs) population transfer from the S_1 state to the electronic ground state S_0 can be observed. For the first ∼30 fs, no transition occurs; apparently, this is the length of time needed to reach the coupling region. For the two solvent modules (toluene, ethanol) the populations of S_0-HT and S_0-CHD are nearly the same, with a slightly higher population of the S_0-HT state after the population transfer is finished. In both cases, a smooth transfer from S_1 to S_0 can be observed. In a solution of pentane, it is generally thought[91,102] that there is 41% conversion of CHD to HT. In vacuum, experimental results indicate are that the yield of hexatriene is almost unity;[91] recent surface hopping studies in vacuum at the XMS-CASPT2 level of theory recover a yield of 47%.[103] The calculations in Figure 5 cannot recover these observations quantitatively—the yield of HT in vacuum being 59% and the solvated yields being less: 51% in both toluene and ethanol. In other words, we do recover the correct trends, but we are off quantitatively. The fact that our vacuum calculations do not match experiment indicates that the problem must involve more than the QM/MM solvent environment; for example, spin-flip TDDFT is known to suffer several problems, with regard to reproducing excited-state crossings and barriers quantitatively.[104] Alternatively, there is always the question of whether or not we should be sampling a Wigner (rather than Boltzmann) distribution with our initial conditions. In any event, qualitatively (although clearly not quantitatively), we do see the expected trend with solvent: the presence of toluene and/or ethanol reduces the yield of HT.

At this point, one would like to understand how the presence of solvent affects the dynamics. As discussed above, the solvent alters the potential energy landscape for the ground state but does not greatly affect the relative excitation energies. Beyond these structural changes, however, the solvent also functions as an energy source and sink, driving and relaxing nonadiabatic transitions—a dynamical feature that is not often fully explored in excited-state nonadiabatic simulations. Of course, solvation and solvent dynamics are very complicated, and one can ask many different questions about such effects: how many molecules drive the downward hop? How many molecules trap the energy? Are some solvent atoms more active than others in driving relaxation? How long does it take for electronic energy to be thermalized? In a future publication, we will analyze the role of solvent in promoting relaxation in a more detailed fashion.

For the moment, within the surface hopping protocol, we note that according to FSSH, an electronic transition between states i and j is promoted by the $\vec{d}_{ij}\cdot\dot{\vec{R}}$ term in eq 7. Thus, of the many questions listed above, the simplest question one can ask is how delocalized are the $\vec{d}_{ij}\cdot\dot{\vec{R}}$ matrix elements? How many molecules actually drive the electronic transition downward for CHD?

This question can be partially answered in the framework of a participation number. For a normalized distribution $\hat{w} = (\hat{w}_1, \hat{w}_2, ..., \hat{w}_N)$ ($\sum_k^N w_k = 1$), the participation number is defined as follows:

$$p_n = \frac{1}{\sum_k^N \hat{w}_k^2} \tag{16}$$

and gives an indication of how many components of the distribution contribute to the whole. Consider the case of N equal weights, $w_i = 1/N$, then $p_n = N$; and contrast with the case where $w_1 = 1$ and all other $w_i = 0$, then $p_n = 1$. The participation number, p_n, may be familiar by way of its relation to the inverse participation ratio, i.p.r. $= p_n/N$, a measure to quantify localization of a wave function on a disordered lattice.[105] In that context, the weights, $\hat{w}_k = c_k^2$, correspond to the expansion coefficients of the wave function, $|\Psi\rangle = \sum_k c_k|k\rangle$.

With this metric in mind, let us consider the quantity $\vec{d}\cdot\dot{\vec{R}}$ for each *atom* in the system during a hopping event. Specifically, we compute

$$w_k = \sqrt{\sum_\gamma (d^{k\gamma}\cdot\dot{R}^{k\gamma})^2} \tag{17}$$

$$\hat{w}_k = \frac{w_k}{\sum_k^N w_k} \tag{18}$$

where $\gamma \in \{x, y, z\}$ indexes the Cartesian coordinates and k indexes all the atoms in the system (CHD, as well as solvent). As defined, p_n gives a qualitative indication of the number of atoms whose motions are driving the electronic transition at each attempted hop. In Figure 6, we plot both the distributions of the energy gap and the *participation number* of $\vec{d}_{ij}\cdot\dot{\vec{R}}$ at the time of a successful hop. Given the lack of a solvatochromatic
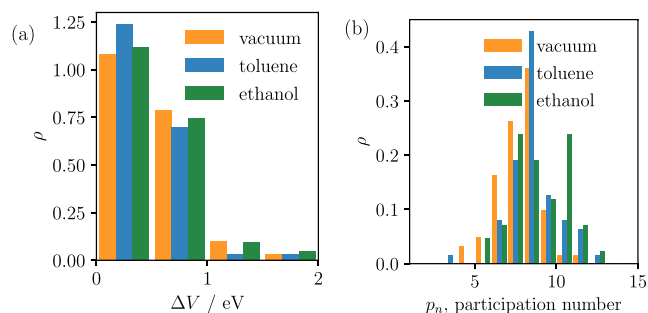
Figure 6. Distribution of successful (downward) hops as quantified by (a) the energy gap and (b) the participation numbers for the nonadiabatic coupling vectors between the S_1 and S_0 state for the three simulations in vacuum, in toluene and in ethanol. As expected a hop is more likely if the energy gap is relatively small. For these successful hops, the distribution of participation number is modestly broader in solvent than in vacuum.
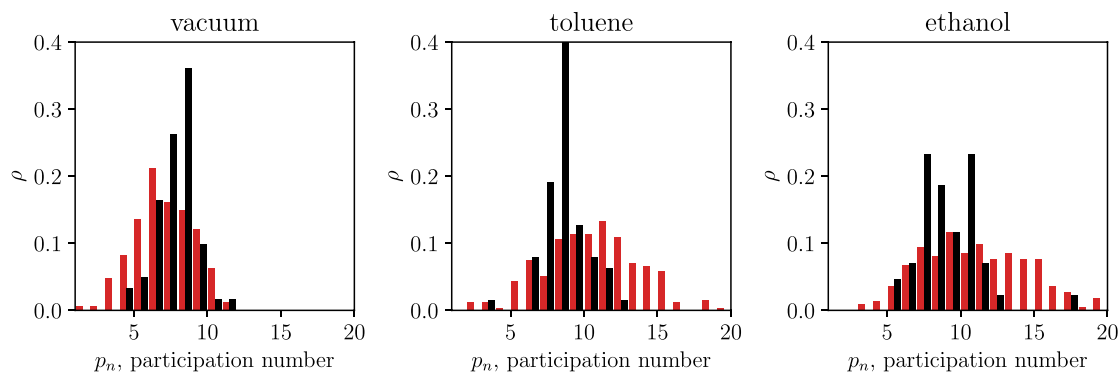
Figure 7. Distribution of successful (black) and failed (red) hops by the participation number of the nonadiabatic coupling vector between the S_1 and S_0 state for the three simulations in vacuum, in toluene and in ethanol. Distributions for successful hops are largely similar to means ± standard deviation: 7.9 ± 1.3 (vacuum), 8.6 ± 1.4 (toluene), and 9.1 ± 2.2 (ethanol). Distributions for frustrated hops are substantially different for the solvated systems: 7.1 ± 2.0 (vacuum), 11.1 ± 4.0 (toluene), and 12.1 ± 5.0 (ethanol).

shift in Figure 3 above, one is perhaps not surprised that the energy gap distribution is largely similar for successful hops in Figure 6a: in all cases, the great majority of hops occur for small energy gaps (<1 eV). More interestingly, however, in Figure 6b, we find that the distribution of the participation ratio is broader and shifted to larger values in a solvent. In other words, the solvent *is* clearly driving the transition downward. Nevertheless, it appears that the solvent is not playing a crucial role; after all, the standard deviation of the participation numbers for successful hops are 1.3 (vacuum), 1.4 (toluene), and 2.8 (ethanol).

Therefore, for now (and within the limitations of a spin-flip electronic structure calculation), we tentatively conclude that the solvent is not driving the photochemical transition of CHD. Instead, our current hypothesis is that the 10% difference in HT yield between the vacuum and solvated environments (highlighted in Figure 5) is the result of differences in vibrational energy dissipation after the hop downward. Such a hypothesis has been motivated by investigating the nature of *frustrated* hops in our simulations. Recall that frustrated hops are the essential ingredient that allows surface hopping to reach thermal equilibrium.

In Figure 7, we compare and contrast the participation number distribution for successful downward hops versus those for frustrated hops. Now, we see a dramatic broadening and shift to larger values in the distribution for frustrated hops when in solvent. In other words, even though the solvent is not driving the electronic transition downward, the solvent is attempting to drive an electronic transition upward; however, the delocalization of vibrational energy within the solvent forbid such a transition (in accordance with the second law of thermodynamics). In a future publication, we will explore, in greater detail, the nature of how the electronic energy is converted to vibrational energy and then delocalized across the solvent.

4. CONCLUSION

We have presented INAQS, an Interface for Non-Adiabatic Quantum mechanics/molecular mechanics in Solvent. Among its demonstrated capabilities are single surface dynamics for the calculation of spectra, ground-state umbrella sampling in a QM/MM framework, and nonadiabatic surface hopping dynamics for studying electronic relaxation processes, when coupled to a large environment. Here, we have studied the CHD molecule, but the most important applications in the

future will no doubt investigate processes with large dipole moments and/or strong system—solvent interactions, especially charge-transfer processes.

■ ASSOCIATED CONTENT

Ⓢ Supporting Information

The Supporting Information is available free of charge at https://pubs.acs.org/doi/10.1021/acs.jctc.2c00204.

Computational details for ground and excited state simulations; notes on performance; additional spectra; practical user input (PDF)

■ AUTHOR INFORMATION

Corresponding Authors

D. Vale Cofer-Shabica − *Department of Chemistry, University of Pennsylvania, Philadelphia, Pennsylvania 19104-6243, United States;* ◉ orcid.org/0000-0003-4623-6521; Email: valecs@sas.upenn.edu

Shirin Faraji − *Zernike Institute for Advanced Materials, Faculty of Science and Engineering, University of Groningen, 9747AG Groningen, The Netherlands;* Email: s.s.faraji@rug.nl

Authors

Maximilian F. S. J. Menger − *Zernike Institute for Advanced Materials, Faculty of Science and Engineering, University of Groningen, 9747AG Groningen, The Netherlands;* ◉ orcid.org/0000-0003-1442-9601

Qi Ou − *AI for Science Institute, Beijing 100080, China*

Yihan Shao − *Department of Chemistry and Biochemistry, University of Oklahoma, Norman, Oklahoma 73019, United States*

Joseph E. Subotnik − *Department of Chemistry, University of Pennsylvania, Philadelphia, Pennsylvania 19104-6243, United States*

Complete contact information is available at:
https://pubs.acs.org/10.1021/acs.jctc.2c00204

Author Contributions

[∇]These authors have contributed equally to this work.

Notes

The authors declare no competing financial interest.

■ REFERENCES

(1) Bannwarth, C.; Caldeweyher, E.; Ehlert, S.; Hansen, A.; Pracht, P.; Seibert, J.; Spicher, S.; Grimme, S. Extended tight-binding quantum chemistry methods. *WIREs Comput. Mol. Sci.* **2021**, *11*, No. e1493.

(2) Datta, D.; Kossmann, S.; Neese, F. Analytic energy derivatives for the calculation of the first-order molecular properties using the domain-based local pair-natural orbital coupled-cluster theory. *J. Chem. Phys.* **2016**, *145*, 114101.

(3) Akimov, A. V.; Prezhdo, O. V. Large-Scale Computations in Chemistry: A Bird's Eye View of a Vibrant Field. *Chem. Rev.* **2015**, *115*, 5797−5890.

(4) Kubař, T.; Welke, K.; Groenhof, G. New QM/MM implementation of the DFTB3 method in the Gromacs package. *J. Comput. Chem.* **2015**, *36*, 1978−1989.

(5) Ufimtsev, I. S.; Martínez, T. J. Quantum Chemistry on Graphical Processing Units. 3. Analytical Energy Gradients, Geometry Optimization, and First Principles Molecular Dynamics. *J. Chem. Theory Comput.* **2009**, *5*, 2619−2628.

(6) Tornai, G. J.; Ladjánszki, I.; Rák, A.; Kis, G.; Cserey, G. Calculation of Quantum Chemical Two-Electron Integrals by Applying Compiler Technology on GPU. *J. Chem. Theory Comput.* **2019**, *15*, 5319−5331.

(7) Frisch, M. J.; Trucks, G. W.; Schlegel, H. B.; Scuseria, G. E.; Robb, M. A.; Cheeseman, J. R.; Scalmani, G.; Barone, V.; Petersson, G. A.; Nakatsuji, H.; Li, X.; Caricato, M.; Marenich, A. V.; Bloino, J.; Janesko, B. G.; Gomperts, R.; Mennucci, B.; Hratchian, H. P.; Ortiz, J. V.; Izmaylov, A. F.; Sonnenberg, J. L.; Williams-Young, D.; Ding, F.; Lipparini, F.; Egidi, F.; Goings, J.; Peng, B.; Petrone, A.; Henderson, T.; Ranasinghe, D.; Zakrzewski, V. G.; Gao, J.; Rega, N.; Zheng, G.; Liang, W.; Hada, M.; Ehara, M.; Toyota, K.; Fukuda, R.; Hasegawa, J.; Ishida, M.; Nakajima, T.; Honda, Y.; Kitao, O.; Nakai, H.; Vreven, T.; Throssell, K.; Montgomery, J. A., Jr.; Peralta, J. E.; Ogliaro, F.; Bearpark, M. J.; Heyd, J. J.; Brothers, E. N.; Kudin, K. N.; Staroverov, V. N.; Keith, T. A.; Kobayashi, R.; Normand, J.; Raghavachari, K.; Rendell, A. P.; Burant, J. C.; Iyengar, S. S.; Tomasi, J.; Cossi, M.; Millam, J. M.; Klene, M.; Adamo, C.; Cammi, R.; Ochterski, J. W.; Martin, R. L.; Morokuma, K.; Farkas, O.; Foresman, J. B.; Fox, D. J. *Gaussian 16*, Revision B.01; Gaussian, Inc.: Wallingford, CT, 2016.

(8) Curutchet, C.; Mennucci, B. Quantum Chemical Studies of Light Harvesting. *Chem. Rev.* **2017**, *117*, 294−343.

(9) Jones, C. M.; List, N. H.; Martínez, T. J. Resolving the ultrafast dynamics of the anionic green fluorescent protein chromophore in water. *Chem. Sci.* **2021**, *12*, 11347−11363.

(10) Zimmer, M. Green Fluorescent Protein (GFP): Applications, Structure, and Related Photophysical Behavior. *Chem. Rev.* **2002**, *102*, 759−782.

(11) Jailaubekov, A. E.; Willard, A. P.; Tritsch, J. R.; Chan, W.-L.; Sai, N.; Gearba, R.; Kaake, L. G.; Williams, K. J.; Leung, K.; Rossky, P. J.; et al. Hot charge-transfer excitons set the time limit for charge separation at donor/acceptor interfaces in organic photovoltaics. *Nature materials* **2013**, *12*, 66−73.

(12) Crespo-Otero, R.; Barbatti, M. Recent Advances and Perspectives on Nonadiabatic Mixed Quantum−Classical Dynamics. *Chem. Rev.* **2018**, *118*, 7026−7068.

(13) Miertuš, S.; Tomasi, J. Approximate evaluations of the electrostatic free energy and internal energy changes in solution processes. *Chem. Phys.* **1982**, *65*, 239−245.

(14) Mennucci, B.; Cammi, R. *Continuum Solvation Models in Chemical Physics: From Theory to Applications*; John Wiley & Sons, Ltd., 2007.

(15) Mennucci, B. Polarizable continuum model. *WIRES Comput. Mol. Sci.* **2012**, *2*, 386−404.

(16) Klamt, A.; Schuurmann, G. COSMO: a new approach to dielectric screening in solvents with explicit expressions for the screening energy and its gradient. *J. Chem. Soc., Perkin Trans.* **1993**, *2*, 799−805.

(17) Pye, C. C.; Ziegler, T. An implementation of the conductor-like screening model of solvation within the Amsterdam density functional package. *Theor. Chem. Acc.* **1999**, *101*, 396−408.

(18) Marenich, A. V.; Cramer, C. J.; Truhlar, D. G. Universal Solvation Model Based on Solute Electron Density and on a Continuum Model of the Solvent Defined by the Bulk Dielectric Constant and Atomic Surface Tensions. *J. Phys. Chem. B* **2009**, *113*, 6378−6396.

(19) Marenich, A. V.; Cramer, C. J.; Truhlar, D. G. Generalized Born Solvation Model SM12. *J. Chem. Theory Comput.* **2013**, *9*, 609−620.

(20) Warshel, A.; Levitt, M. Theoretical studies of enzymic reactions: Dielectric, electrostatic and steric stabilization of the carbonium ion in the reaction of lysozyme. *J. Mol. Biol.* **1976**, *103*, 227−249.

(21) Maseras, F.; Morokuma, K. IMOMM: A new integrated ab initio + molecular mechanics geometry optimization scheme of equilibrium structures and transition states. *J. Comput. Chem.* **1995**, *16*, 1170−1179.

(22) Svensson, M.; Humbel, S.; Froese, R. D. J.; Matsubara, T.; Sieber, S.; Morokuma, K. ONIOM: A Multilayered Integrated MO + MM Method for Geometry Optimizations and Single Point Energy Predictions. A Test for Diels-Alder Reactions and Pt$(P(t-Bu)_3)_2$ + H$_2$ Oxidative Addition. *J. Phys. Chem.* **1996**, *100*, 19357−19363.

(23) Dapprich, S.; Komáromi, I.; Byun, K.; Morokuma, K.; Frisch, M. J. A new ONIOM implementation in Gaussian98. Part I. The calculation of energies, gradients, vibrational frequencies and electric field derivatives. *J. Mol. Struct.* **1999**, *461−462*, 1−21.

(24) Vreven, T.; Morokuma, K. Hybrid Methods: ONIOM-(QM:MM) and QM/MM. In *Annual Reports in Computational Chemistry*, Vol. *2*; Spellmeyer, D. C., Ed.; Elsevier, 2006; Chapter 3, pp 35−51.

(25) Lin, H.; Truhlar, D. G. QM/MM: what have we learned, where are we, and where do we go from here? *Theor. Chem. Acc.* **2007**, *117*, 185.

(26) Groenhof, G. In *Biomolecular Simulations: Methods and Protocols*; Monticelli, L., Salonen, E., Eds.; Humana Press: Totowa, NJ, 2013; pp 43−66.

(27) Loco, D.; Polack, É.; Caprasecca, S.; Lagardère, L.; Lipparini, F.; Piquemal, J.-P.; Mennucci, B. A QM/MM Approach Using the AMOEBA Polarizable Embedding: From Ground State Energies to Electronic Excitations. *J. Chem. Theory Comput.* **2016**, *12*, 3654−3661.

(28) Lin, H.; Truhlar, D. G. Redistributed Charge and Dipole Schemes for Combined Quantum Mechanical and Molecular Mechanical Calculations. *J. Phys. Chem. A* **2005**, *109*, 3991−4004.

(29) Zhang, Y.; Lin, H.; Truhlar, D. G. Self-Consistent Polarization of the Boundary in the Redistributed Charge and Dipole Scheme for Combined Quantum-Mechanical and Molecular-Mechanical Calculations. *J. Chem. Theory Comput.* **2007**, *3*, 1378−1398.

(30) Boulanger, E.; Thiel, W. Solvent Boundary Potentials for Hybrid QM/MM Computations Using Classical Drude Oscillators: A Fully Polarizable Model. *J. Chem. Theory Comput.* **2012**, *8*, 4527−4538.

(31) Epifanovsky, E.; Gilbert, A. T. B.; Feng, X.; Lee, J.; Mao, Y.; Mardirossian, N.; Pokhilko, P.; White, A. F.; Coons, M. P.; Dempwolff, A. L.; Gan, Z.; Hait, D.; Horn, P. R.; Jacobson, L. D.; Kaliman, I.; Kussmann, J.; Lange, A. W.; Lao, K. U.; Levine, D. S.; Liu, J.; McKenzie, S. C.; Morrison, A. F.; Nanda, K. D.; Plasser, F.; Rehn, D. R.; Vidal, M. L.; You, Z.-Q.; Zhu, Y.; Alam, B.; Albrecht, B. J.; Aldossary, A.; Alguire, E.; Andersen, J. H.; Athavale, V.; Barton, D.; Begam, K.; Behn, A.; Bellonzi, N.; Bernard, Y. A.; Berquist, E. J.; Burton, H. G. A.; Carreras, A.; Carter-Fenk, K.; Chakraborty, R.; Chien, A. D.; Closser, K. D.; Cofer-Shabica, V.; Dasgupta, S.; de Wergifosse, M.; Deng, J.; Diedenhofen, M.; Do, H.; Ehlert, S.; Fang, P.-T.; Fatehi, S.; Feng, Q.; Friedhoff, T.; Gayvert, J.; Ge, Q.; Gidofalvi, G.; Goldey, M.; Gomes, J.; González-Espinoza, C. E.; Gulania, S.; Gunina, A. O.; Hanson-Heine, M. W. D.; Harbach, P. H. P.; Hauser, A.; Herbst, M. F.; Hernández Vera, M.; Hodecker, M.; Holden, Z. C.; Houck, S.; Huang, X.; Hui, K.; Huynh, B. C.; Ivanov, M.; Jász, A.; Ji, H.; Jiang, H.; Kaduk, B.; Kähler, S.; Khistyaev, K.; Kim, J.; Kis, G.; Klunzinger, P.; Koczor-Benda, Z.; Koh, J. H.; Kosenkov, D.; Koulias, L.; Kowalczyk, T.; Krauter, C. M.; Kue, K.; Kunitsa, A.; Kus, T.; Ladjánszki, I.; Landau, A.; Lawler, K. V.; Lefrancois, D.; Lehtola, S.; Li, R. R.; Li, Y.-P.; Liang, J.; Liebenthal, M.; Lin, H.-H.; Lin, Y.-S.; Liu, F.; Liu, K.-Y.; Loipersberger, M.; Luenser, A.; Manjanath, A.; Manohar, P.; Mansoor, E.; Manzer, S. F.; Mao, S.-P.; Marenich, A. V.; Markovich, T.; Mason, S.; Maurer, S. A.; McLaughlin, P. F.; Menger, M. F. S. J.; Mewes, J.-M.; Mewes, S. A.; Morgante, P.; Mullinax, J. W.; Oosterbaan, K. J.; Paran, G.; Paul, A. C.; Paul, S. K.; Pavošević, F.; Pei, Z.; Prager, S.; Proynov, E. I.; Rák, A.; Ramos-Cordoba, E.; Rana, B.; Rask, A. E.; Rettig, A.; Richard, R. M.; Rob, F.; Rossomme, E.; Scheele, T.; Scheurer, M.; Schneider, M.; Sergueev, N.; Sharada, S. M.; Skomorowski, W.; Small, D. W.; Stein, C. J.; Su, Y.-C.; Sundstrom, E. J.; Tao, Z.; Thirman, J.; Tornai, G. J.; Tsuchimochi, T.; Tubman, N. M.; Veccham, S. P.; Vydrov, O.; Wenzel, J.; Witte, J.; Yamada, A.; Yao, K.; Yeganeh, S.; Yost, S. R.; Zech, A.; Zhang, I. Y.; Zhang, X.; Zhang, Y.; Zuev, D.; Aspuru-Guzik, A.; Bell, A. T.; Besley, N. A.; Bravaya, K. B.; Brooks, B. R.; Casanova, D.; Chai, J.-D.; Coriani, S.; Cramer, C. J.; Cserey, G.; DePrince, A. E.; DiStasio, R. A.; Dreuw, A.; Dunietz, B. D.; Furlani, T. R.; Goddard, W. A.; Hammes-Schiffer, S.; Head-Gordon, T.; Hehre, W. J.; Hsu, C.-P.; Jagau, T.-C.; Jung, Y.; Klamt, A.; Kong, J.; Lambrecht, D. S.; Liang, W.; Mayhall, N. J.; McCurdy, C. W.; Neaton, J. B.; Ochsenfeld, C.; Parkhill, J. A.; Peverati, R.; Rassolov, V. A.; Shao, Y.; Slipchenko, L. V.; Stauch, T.; Steele, R. P.; Subotnik, J. E.; Thom, A. J. W.; Tkatchenko, A.; Truhlar, D. G.; Van Voorhis, T.; Wesolowski, T. A.; Whaley, K. B.; Woodcock, H. L.; Zimmerman, P. M.; Faraji, S.; Gill, P. M. W.; Head-Gordon, M.; Herbert, J. M.; Krylov, A. I. Software for the frontiers of quantum chemistry: An overview of developments in the Q-Chem 5 package. *J. Chem. Phys.* **2021**, *155*, 084801.

(32) Kästner, J.; Thiel, S.; Senn, H. M.; Sherwood, P.; Thiel, W. Exploiting QM/MM Capabilities in Geometry Optimization: A Microiterative Approach Using Electrostatic Embedding. *J. Chem. Theory Comput.* **2007**, *3*, 1064−1072.

(33) Pronk, S.; Páll, S.; Schulz, R.; Larsson, P.; Bjelkmar, P.; Apostolov, R.; Shirts, M. R.; Smith, J. C.; Kasson, P. M.; van der Spoel, D.; Hess, B.; Lindahl, E. GROMACS 4.5: a high-throughput and highly parallel open source molecular simulation toolkit. *Bioinformatics* **2013**, *29*, 845−854.

(34) Melo, M. C. R.; Bernardi, R. C.; Rudack, T.; Scheurer, M.; Riplinger, C.; Phillips, J. C.; Maia, J. D. C.; Rocha, G. B.; Ribeiro, J. V.; Stone, J. E.; Neese, F.; Schulten, K.; Luthey-Schulten, Z. NAMD Goes Quantum: an Integrative Suite for Hybrid Simulations. *Nat. Methods* **2018**, *15*, 351−354.

(35) Walker, R. C.; Crowley, M. F.; Case, D. A. The implementation of a fast and accurate QM/MM potential method in Amber. *J. Comput. Chem.* **2008**, *29*, 1019−1031.

(36) Götz, A. W.; Clark, M. A.; Walker, R. C. An extensible interface for QM/MM molecular dynamics simulations with AMBER. *J. Comput. Chem.* **2014**, *35*, 95−108.

(37) Brooks, B. R.; Brooks, C. L., III; Mackerell, A. D., Jr.; Nilsson, L.; Petrella, R. J.; Roux, B.; Won, Y.; Archontis, G.; Bartels, C.; Boresch, S.; Caflisch, A.; Caves, L.; Cui, Q.; Dinner, A. R.; Feig, M.; Fischer, S.; Gao, J.; Hodoscek, M.; Im, W.; Kuczera, K.; Lazaridis, T.; Ma, J.; Ovchinnikov, V.; Paci, E.; Pastor, R. W.; Post, C. B.; Pu, J. Z.; Schaefer, M.; Tidor, B.; Venable, R. M.; Woodcock, H. L.; Wu, X.; Yang, W.; York, D. M.; Karplus, M. CHARMM: The biomolecular simulation program. *J. Comput. Chem.* **2009**, *30*, 1545−1614.

(38) Sherwood, P.; de Vries, A. H.; Guest, M. F.; Schreckenbach, G.; Catlow, C. R. A.; French, S. A.; Sokol, A. A.; Bromley, S. T.; Thiel, W.; Turner, A. J.et al.QUASI: A general purpose implementation of the QM/MM approach and its application to problems in catalysis. *J. Mol. Struct.: THEOCHEM* **2003**, *632*, 1−28.

(39) Metz, S.; Kästner, J.; Sokol, A. A.; Keal, T. W.; Sherwood, P. ChemShell—a modular software package for QM/MM simulations. *WIREs Comput. Mol. Sci.* **2014**, *4*, 101−110.

(40) Lu, Y.; Farrow, M. R.; Fayon, P.; Logsdail, A. J.; Sokol, A. A.; Catlow, C. R. A.; Sherwood, P.; Keal, T. W. Open-Source, Python-Based Redevelopment of the ChemShell Multiscale QM/MM Environment. *J. Chem. Theory Comput.* **2019**, *15*, 1317−1328.

(41) Altoe, P.; Stenta, M.; Bottoni, A.; Garavelli, M.; Maroulis, G.; Simos, T. E. COBRAMM: A Tunable QM/MM Approach to Complex Molecular Architectures. Modelling the Excited and Ground State Properties of Sized Molecular Systems. *AIP Conf. Proc.* **2007**, *963*, 491−505.

(42) Weingart, O.; Nenov, A.; Altoè, P.; Rivalta, I.; Segarra-Martí, J.; Dokukina, I.; Garavelli, M. COBRAMM 2.0 — A software interface for tailoring molecular electronic structure calculations and running nanoscale (QM/MM) simulations. *J. Mol. Model.* **2018**, *24*, 271.

(43) Lin, H.; Zhang, Y.; Pezeshki, S.; Wang, B.; Wu, X.-P.; Gagliardi, L.; Truhlar, D. *QMMM 2018*; University of Minnesota: Minneapolis, MN, USA, 2018,.

(44) Richter, M.; Marquetand, P.; González-Vázquez, J.; Sola, I.; González, L. SHARC: ab initio Molecular Dynamics with Surface Hopping in the Adiabatic Representation Including Arbitrary Couplings. *J. Chem. Theory Comput.* **2011**, *7*, 1253−1258.

(45) Mai, S.; Marquetand, P.; González, L. Nonadiabatic Dynamics: The SHARC Approach. *WIREs Comput. Mol. Sci.* **2018**, *8*, No. e1370.

(46) Barbatti, M.; Ruckenbauer, M.; Plasser, F.; Pittner, J.; Granucci, G.; Persico, M.; Lischka, H. Newton-X: a surface-hopping program for nonadiabatic molecular dynamics. *WIREs Computational Molecular Science* **2014**, *4*, 26−33.

(47) Ruckenbauer, M.; Barbatti, M.; Müller, T.; Lischka, H. Nonadiabatic Excited-State Dynamics with Hybrid ab Initio Quantum-Mechanical/Molecular-Mechanical Methods: Solvation of the Pentadieniminium Cation in Apolar Media. *J. Phys. Chem. A* **2010**, *114*, 6757−6765.

(48) Cui, G.; Thiel, W. Generalized trajectory surface-hopping method for internal conversion and intersystem crossing. *J. Chem. Phys.* **2014**, *141*, 124101.

(49) Granucci, G.; Persico, M. Excited state dynamics with the direct trajectory surface hopping method: azobenzene and its derivatives as a case study. *Theor. Chem. Acc.* **2007**, *117*, 1131−1143.

(50) Lan, Z.; Lu, Y.; Fabiano, E.; Thiel, W. QM/MM Nonadiabatic Decay Dynamics of 9H-Adenine in Aqueous Solution. *ChemPhysChem* **2011**, *12*, 1989−1998.

(51) Avagliano, D.; Bonfanti, M.; Garavelli, M.; González, L. QM/MM Nonadiabatic Dynamics: the SHARC/COBRAMM Approach. *J. Chem. Theory Comp.* **2021**, *17*, 4639−4647.

(52) Menger, M. F. S. J.; Plasser, F.; Mennucci, B.; González, L. Surface hopping within an exciton picture - An electrostatic embedding scheme. *J. Chem. Theory Comput.* **2018**,.146139

(53) Persico, M.; Granucci, G. An overview of nonadiabatic dynamics simulations methods, with focus on the direct approach versus the fitting of potential energy surfaces. *Theor. Chem. Acc.* **2014**, *133*, 1526.

(54) Groenhof, G.; Bouxin-Cademartory, M.; Hess, B.; de Visser, S. P.; Berendsen, H. J. C.; Olivucci, M.; Mark, A. E.; Robb, M. A. Photoactivation of the Photoactive Yellow Protein: Why Photon Absorption Triggers a Trans-to-Cis Isomerization of the Chromophore in the Protein. *J. Am. Chem. Soc.* **2004**, *126*, 4228−4233.

(55) Morozov, D.; Groenhof, G. Photobiology in action: excited-state QM/MM simulations for understanding photodynamics in biological systems. In *Abstracts of Papers of the American Chemical Society*; American Chemical Society: Washington, DC, 2016.

(56) Tavernelli, I.; Curchod, B. F.; Rothlisberger, U. Nonadiabatic molecular dynamics with solvent effects: A LR-TDDFT QM/MM study of ruthenium (II) tris (bipyridine) in water. *Chem. Phys.* **2011**, *391*, 101−109.

(57) Miertuš, S.; Scrocco, E.; Tomasi, J. Electrostatic interaction of a solute with a continuum. A direct utilizaion of AB initio molecular potentials for the prevision of solvent effects. *Chem. Phys.* **1981**, *55*, 117−129.

(58) Senn, H. M.; Thiel, W. QM/MM methods for biomolecular systems. *Angew. Chem.* **2009**, *48*, 1198−1229.

(59) Gehlen, J. N.; Chandler, D.; Kim, H. J.; Hynes, J. T. Free energies of electron transfer. *J. Phys. Chem.* **1992**, *96*, 1748−1753.

(60) Tully, J. C. Molecular dynamics with electronic transitions. *J. Chem. Phys.* **1990**, *93*, 1061−1071.

(61) Doltsinis, N. In *Quantum Simulations of Complex Many-Body Systems: From Theory to Algorithms*; Grotendorst, J., Marx, D., Muramatsu, A., Eds.; John von Neumann Institute of Computation, 2002; pp 377−397.

(62) Jasper, A. W.; Truhlar, D. G. In *Conical Intersections: Theory, Computation and Experiment*; Domcke, W., Yarkony, D. R., Koppel, H., Eds.; World Scientific Publishing Co.: NJ, 2011; pp 375−414.

(63) Bellonzi, N.; Jain, A.; Subotnik, J. E. An assessment of mean-field mixed semiclassical approaches: Equilibrium populations and algorithm stability. *J. Chem. Phys.* **2016**, *144*, 154110.

(64) Chen, H.-T.; Li, T. E.; Sukharev, M.; Nitzan, A.; Subotnik, J. E. Ehrenfest+R dynamics. I. A mixed quantum−classical electrodynamics simulation of spontaneous emission. *J. Chem. Phys.* **2019**, *150*, 044102.

(65) Meyer, H. D.; Miller, W. H. A classical analog for electronic degrees of freedom in nonadiabatic collision processes. *J. Chem. Phys.* **1979**, *70*, 3214.

(66) Kim, H.; Nassimi, A.; Kapral, R. Quantum-classical liouville dynamics in the mapping basis. *J. Chem. Phys.* **2008**, *129*, 084102.

(67) Cotton, S. J.; Igumenshchev, K.; Miller, W. H. Symmetrical windowing for quantum states in quasi-classical trajectory simulations: Application to electron transfer. *J. Chem. Phys.* **2014**, *141*, 084104.

(68) Parandekar, P. V.; Tully, J. C. Mixed quantum-classical equilibrium. *J. Chem. Phys.* **2005**, *122*, 094102.

(69) Schmidt, J. R.; Parandekar, P. V.; Tully, J. C. Mixed quantum-classical equilibrium: Surface hopping. *J. Chem. Phys.* **2008**, *129*, 044104.

(70) Miller, W. H.; Cotton, S. J. Communication: Note on detailed balance in symmetrical quasi-classical models for electronically non-adiabatic dynamics. *J. Chem. Phys.* **2015**, *142*, 131103.

(71) Jain, A.; Alguire, E.; Subotnik, J. E. An Efficient, Augmented Surface Hopping Algorithm That Includes Decoherence for Use in Large-Scale Simulations. *J. Chem. Theory Comput.* **2016**, *12*, 5256−5268.

(72) Meek, G. A.; Levine, B. G. Evaluation of the Time-Derivative Coupling for Accurate Electronic State Transition Probabilities from Numerical Simulations. *J. Phys. Chem. Lett.* **2014**, *5*, 2351−2356.

(73) Hammes-Schiffer, S.; Tully, J. C. Proton transfer in solution: Molecular dynamics with quantum transitions. *J. Chem. Phys.* **1994**, *101*, 4657−4667.

(74) Pittner, J.; Lischka, H.; Barbatti, M. Optimization of mixed quantum-classical dynamics: Time-derivative coupling terms and selected couplings. *Chem. Phys.* **2009**, *356*, 147−152.

(75) Loring, T. A. Computing a logarithm of a unitary matrix with general spectrum. *Numerical Linear Algebra with Applications* **2014**, *21*, 744−760.

(76) Chen, H.-T.; Chen, J.; Cofer-Shabica, D. V.; Zhou, Z.; Athavale, V.; Medders, G.; Menger, M.; Subotnik, J.; Jin, Z. Methods to Calculate Electronic Excited-state Dynamics For Molecules on Large Metal Clusters with Many States: Ensuring Fast Overlap

Calculations and a Robust Choice of Phase. *J. Chem. Theory Comput.* **2022**, *18* (6), 3296−3307.

(77) Zhou, Z.; Jin, Z.; Qiu, T.; Rappe, A. M.; Subotnik, J. E. A Robust and Unified Solution for Choosing the Phases of Adiabatic States as a Function of Geometry: Extending Parallel Transport Concepts to the Cases of Trivial and Near-Trivial Crossings. *J. Chem. Theory Comput.* **2020**, *16*, 835−846.

(78) Lee, E. M. Y.; Willard, A. P. Solving the Trivial Crossing Problem While Preserving the Nodal Symmetry of the Wave Function. *J. Chem. Theory Comput.* **2019**, *15*, 4332−4343.

(79) Jasper, A. W.; Truhlar, D. G. Improved treatment of momentum at classically forbidden electronic transitions in trajectory surface hopping calculations. *Chem. Phys. Lett.* **2003**, *369*, 60−67.

(80) Jain, A. Professor, IIT Bombay. Personal communication, 2020.

(81) Landry, B. R.; Subotnik, J. E. Standard surface hopping predicts incorrect scaling for Marcus' golden-rule rate: The decoherence problem cannot be ignored. *J. Chem. Phys.* **2011**, *135*, 191101.

(82) Chen, H.-T.; Reichman, D. R. On the accuracy of surface hopping dynamics in condensed phase non-adiabatic problems. *J. Chem. Phys.* **2016**, *144*, 094104.

(83) Jain, A.; Subotnik, J. E. Does Nonadiabatic Transition State Theory Make Sense Without Decoherence? *J. Phys. Chem. Lett.* **2015**, *6*, 4809−4814.

(84) Sisto, A.; Glowacki, D. R.; Martínez, T. J. Ab Initio Nonadiabatic Dynamics of Multichromophore Complexes: A Scalable Graphical-Processing-Unit-Accelerated Exciton Framework. *Acc. Chem. Res.* **2014**, *47*, 2857−2866.

(85) Sisto, A.; Stross, C.; van der Kamp, M. W.; O'Connor, M.; McIntosh-Smith, S.; Johnson, G. T.; Hohenstein, E. G.; Manby, F. R.; Glowacki, D. R.; Martínez, T. J. Atomistic non-adiabatic dynamics of the LH2 complex with a GPU-accelerated ab initio exciton model. *Phys. Chem. Chem. Phys.* **2017**, *19*, 14924−14936.

(86) Gil, E. S.; Granucci, G.; Persico, M. Surface Hopping Dynamics with the Frenkel Exciton Model in a Semiempirical Framework. *J. Chem. Theory Comput.* **2021**, *17*, 7373−7383.

(87) Pechukas, P. Time-Dependent Semiclassical Scattering Theory. II. Atomic Collisions. *Phys. Rev.* **1969**, *181*, 174.

(88) Herman, M. F. Nonadiabatic semiclassical scattering. I. Analysis of generalized surface hopping procedures. *J. Chem. Phys.* **1984**, *81*, 754−763.

(89) Allen, M.; Tildesley, D. *Computer Simulation of Liquids*; Clarendon Press, 1989.

(90) Tribello, G. A.; Bonomi, M.; Branduardi, D.; Camilloni, C.; Bussi, G. PLUMED 2: New feathers for an old bird. *Comput. Phys. Commun.* **2014**, *185*, 604−613.

(91) Deb, S.; Weber, P. M. The Ultrafast Pathway of Photon-Induced Electrocyclic Ring-Opening Reactions: The Case of 1,3-Cyclohexadiene. *Annu. Rev. Phys. Chem.* **2011**, *62*, 19−39.

(92) Trulson, M. O.; Dollinger, G. D.; Mathies, R. A. Femtosecond photochemical ring opening dynamics of 1, 3-cyclohexadiene from resonance Raman intensities. *J. Am. Chem. Soc.* **1987**, *109*, 586−587.

(93) Rudakov, F.; Weber, P. M. Ground state recovery and molecular structure upon ultrafast transition through conical intersections in cyclic dienes. *Chem. Phys. Lett.* **2009**, *470*, 187−190.

(94) Kuthirummal, N.; Rudakov, F. M.; Evans, C. L.; Weber, P. M. Spectroscopy and femtosecond dynamics of the ring opening reaction of 1,3-cyclohexadiene. *J. Chem. Phys.* **2006**, *125*, 133307.

(95) Garavelli, M.; Page, C. S.; Celani, P.; Olivucci, M.; Schmid, W. E.; Trushin, S. A.; Fuss, W. Reaction Path of a sub-200 fs Photochemical Electrocyclic Reaction. *J. Phys. Chem. A* **2001**, *105*, 4458−4469.

(96) Merchán, M.; Serrano-Andrés, L.; Slater, L. S.; Roos, B. O.; McDiarmid, R.; Xing. Electronic Spectra of 1,4-Cyclohexadiene and 1,3-Cyclohexadiene: A Combined Experimental and Theoretical Investigation. *J. Phys. Chem. A* **1999**, *103*, 5468−5476.

(97) Tamura, H.; Nanbu, S.; Ishida, T.; Nakamura, H. Ab initio nonadiabatic quantum dynamics of cyclohexadiene/hexatriene ultra-fast photoisomerization. *J. Chem. Phys.* **2006**, *124*, 084313.

(98) Furche, F.; Ahlrichs, R.; Hättig, C.; Klopper, W.; Sierka, M.; Weigend, F. Turbomole. *WIREs Comput. Mol. Sci.* **2014**, *4*, 91−100.

(99) Chandler, D. *Introduction to Modern Statistical Mechanics*; Oxford University Press, 1987.

(100) Hub, J. S.; de Groot, B. L.; van der Spoel, D. g_wham—A Free Weighted Histogram Analysis Implementation Including Robust Error and Autocorrelation Estimates. *J. Chem. Theory Comput.* **2010**, *6*, 3713−3720.

(101) Zhang, X.; Herbert, J. M. Spin-flip, tensor equation-of-motion configuration interaction with a density-functional correction: A spin-complete method for exploring excited-state potential energy surfaces. *J. Chem. Phys.* **2015**, *143*, 234107.

(102) Minnaard, N. G.; Havinga, E. Some aspects of the solution photochemistry of 1,3-cyclohexadiene, (Z)- and (E)-1,3,5-hexatriene. *Rec. Trav. Chim. Pays-Bas* **1973**, *92*, 1315−1320.

(103) Polyak, I.; Hutton, L.; Crespo-Otero, R.; Barbatti, M.; Knowles, P. J. Ultrafast Photoinduced Dynamics of 1,3-Cyclohexadiene Using XMS-CASPT2 Surface Hopping. *J. Chem. Theory Comput.* **2019**, *15*, 3929−3940.

(104) Casanova, D.; Head-Gordon, M. The spin-flip extended single excitation configuration interaction method. *J. Chem. Phys.* **2008**, *129*, 064104.

(105) Weaire, D.; Williams, A. R. New numerical approach to the Anderson localization problem. *J. Phys. C: Solid State Phys.* **1976**, *9*, L461−L463.

📖 Recommended by ACS

Recent Advances in First-Principles Based Molecular Dynamics

François Mouvet, Ursula Rothlisberger, *et al.*

JANUARY 13, 2022
ACCOUNTS OF CHEMICAL RESEARCH

READ ☑

ReaxFF/AMBER—A Framework for Hybrid Reactive/Nonreactive Force Field Molecular Dynamics Simulations

Ali Rahnamoun, Hasan Metin Aktulga, *et al.*

NOVEMBER 03, 2020
JOURNAL OF CHEMICAL THEORY AND COMPUTATION

READ ☑

Accelerating *Ab Initio* Quantum Mechanical and Molecular Mechanical (QM/MM) Molecular Dynamics Simulations with Multiple Time Step Integration and a Recalibrated S...

Xiaoliang Pan, Yihan Shao, *et al.*

JUNE 02, 2022
THE JOURNAL OF PHYSICAL CHEMISTRY B

READ ☑

Using Atomic Confining Potentials for Geometry Optimization and Vibrational Frequency Calculations in Quantum-Chemical Models of Enzyme Active Sites

Saswata Dasgupta and John M. Herbert

JANUARY 27, 2020
THE JOURNAL OF PHYSICAL CHEMISTRY B

READ ☑

Get More Suggestions >